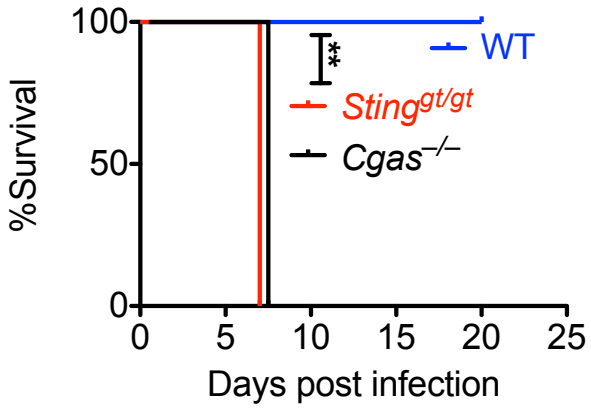

Figure S1. Validation of *Cgas*$^{-/-}$ mice. Related to Figure 4.
WT, *Sting*$^{gt/gt}$, *Cgas*$^{-/-}$ mice were infected with 10^7 PFU HSV-1 intravenously, and monitored for survival. Statistical analysis was assessed using the log-rank test. Results are representative of two independent experiments.

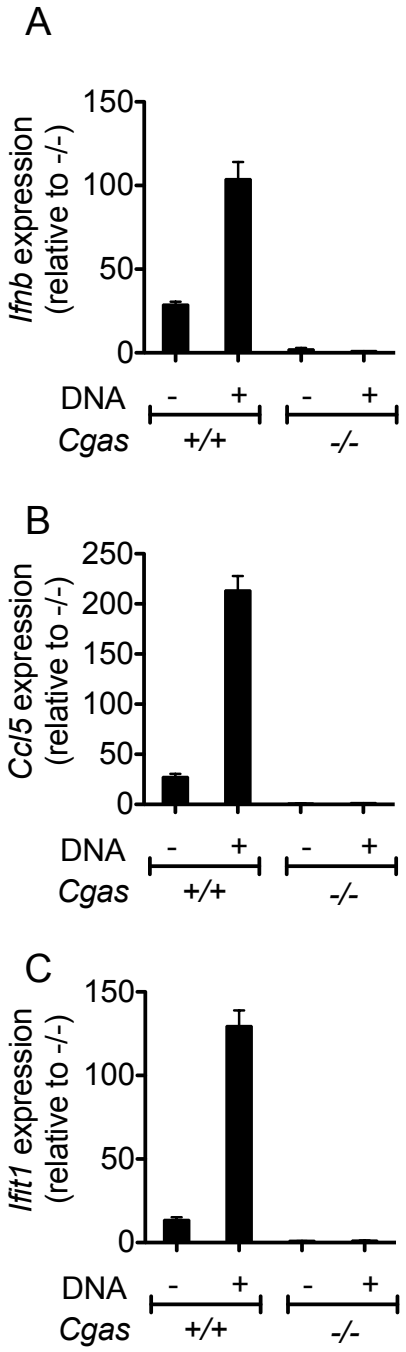

Figure S2. Validation of B16 *Cgas*$^{-/-}$ tumor cells. Related to Figure 6.
B16-*Cgas*$^{+/+}$ and B16-*Cgas*$^{-/-}$ cells were transfected with HT-DNA, and assayed for *Ifnb, Ccl5 and Ifit1* gene expression using Q-RT-PCR. Fold expression is shown relative to *Cgas*$^{-/-}$ cells. Results are representative of two to four independent experiments, and data consist of three technical replicates. Bars represent means +/- SEM.

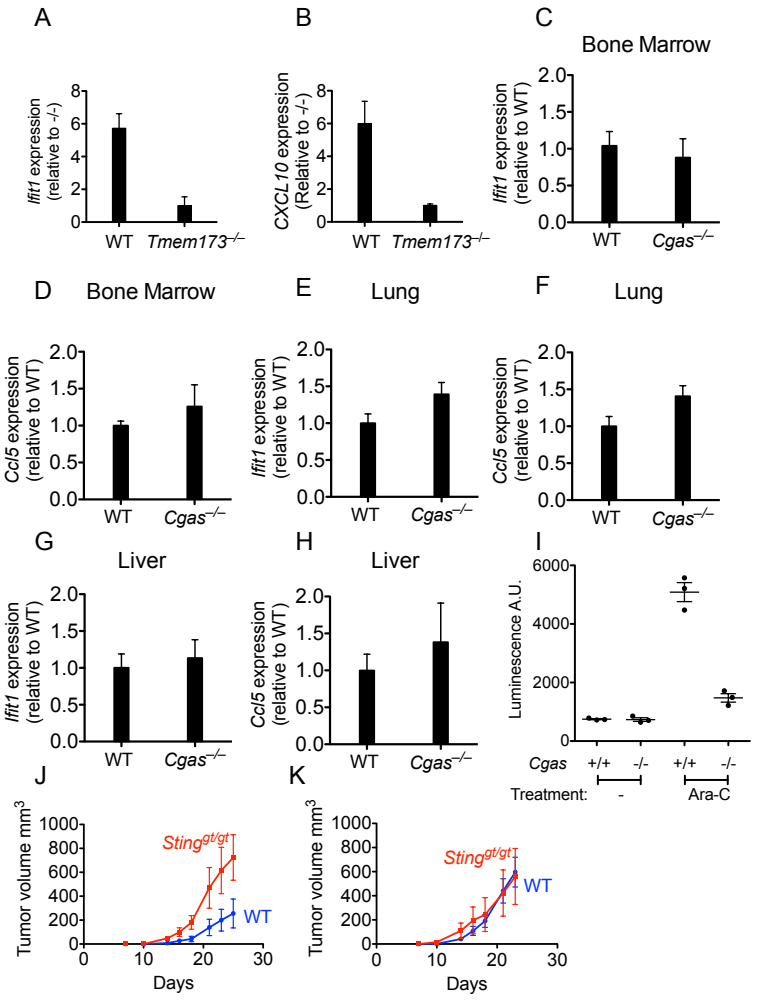

Figure S3. Activation of CGAS-STING in tumors *in vitro* and *in vivo.* Related to Figure 6.

(**A-B**) QRT-PCR analysis of *IFIT1* (**A**) and *CXCL10* (**B**) expression levels in THP1-*TMEM173*$^{+/+}$, and THP1-*TMEM173*$^{-/-}$ tumor cells. Results are representative of two independent experiments, and data consist of three technical replicates. QRT-PCR analysis of *Ccl5* and *Ifit1* expression levels in bone marrow (**C-D**), Lung (**E-F**), and Liver (**G-H**) cells isolated from WT or *Cgas*$^{-/-}$ mice (**I**) B16-*Cgas*$^{+/+}$ and B16-*Cgas*$^{-/-}$ cells were incubated in media with or without 50μM ARA-C, and after 48 hours secreted type I IFN was measured using an IFN bioassay. Tumor cells (10^5) were injected s.c. into WT or *Sting*$^{gt/gt}$ mice and tumor growth monitored as in Fig. 1 legend. Each group contained 4-6 mice, and results are representative of two independent experiments. Injected tumor cells were: B16-BL6-*Cgas*$^{-/-}$ cells transduced with active (*Cgas*^{wt}, **J**), or inactive (*Cgas*^{mut}, **K**) CGAS expression vector. Bars represent means +/- SEM. Statistical analysis was done as in Fig. 1.

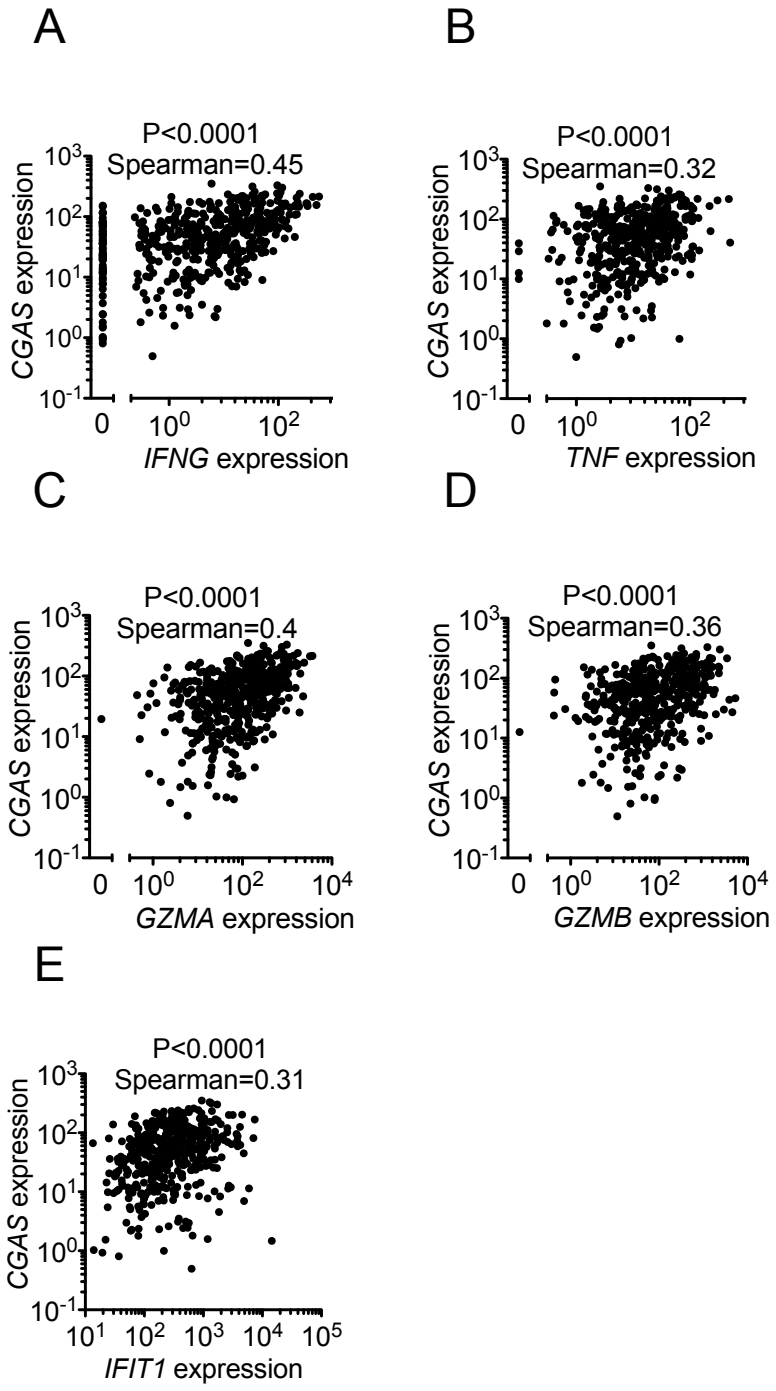

Figure S4. Correlation between CGAS expression and immune activation in melanoma patients. Related to Figure 7. Plots of expression of *CGAS* expression versus the immune activation markers *IFNG* (**A**), *TNF* (**B**), *GZMA* (**C**), *GZMB* (**D**), and *IFIT1* (**E**). All data were obtained from TCGA using the cbioportal website. Statistical correlation was assessed using the Spearman coefficient.

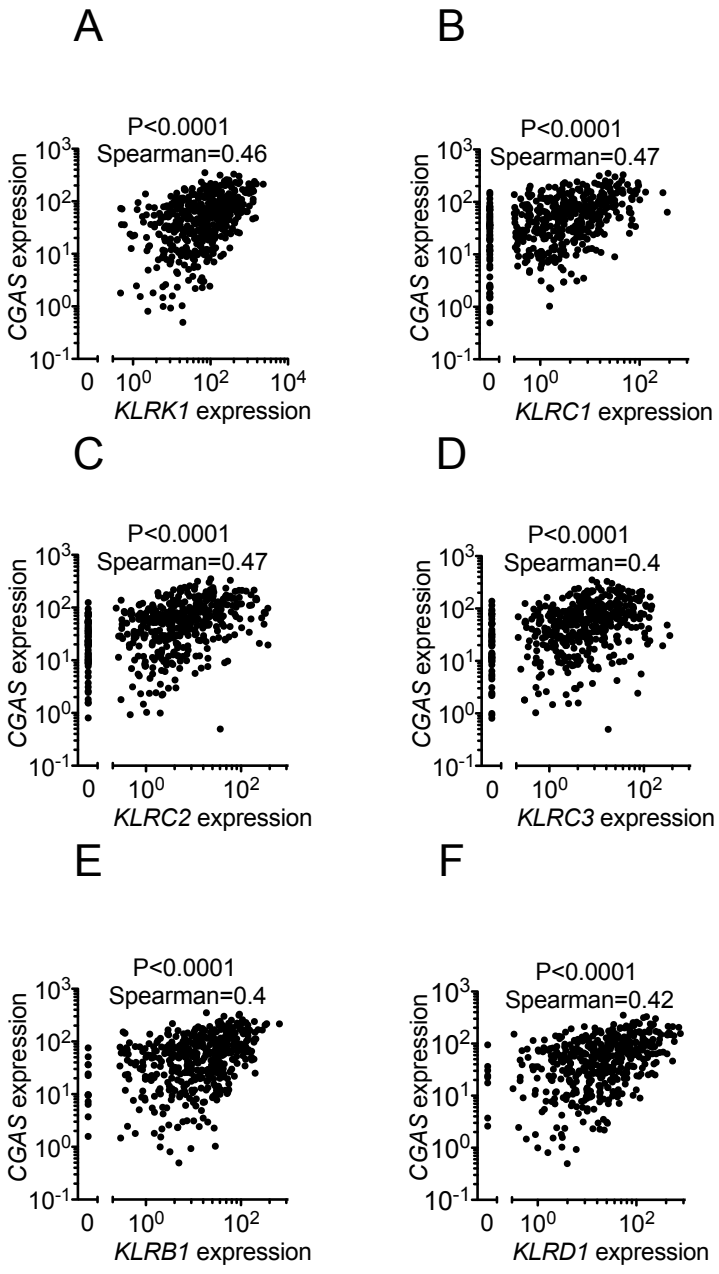

Figure S5. Correlation between CGAS expression and NK cell infiltration in melanoma patients. Related to Figure 7. Plots of expression of *CGAS* expression versus expression of the NK cell receptors *KLRK1* (**A**), *KLRC1* (**B**), *KLRC2* (**C**), *KLRC3* (**D**), *KLRB1* (**E**), and *KLRD1* (**F**). All data were obtained from TCGA using the cbioportal website. Statistical correlation was assessed using the Spearman coefficient.

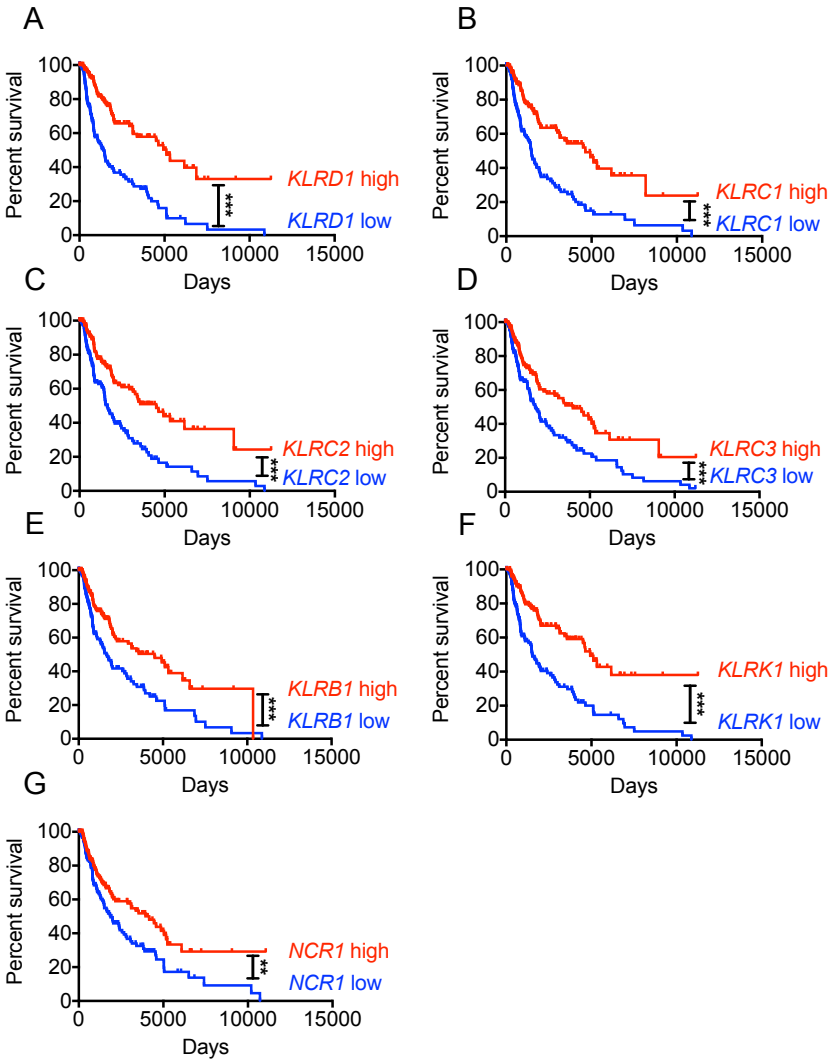

Figure S6. Correlation between NK cell infiltration and survival in melanoma patients. Related to Figure 7. Kaplan-Meier plots of melanoma patient survival. Patients were segmented by expression (highest and lowest thirds) of various NK cell receptors: *KLRD1* (**A**), *KLRC1* (**B**), *KLRC2* (**C**), *KLRC3* (**D**), *KLRB1* (**E**), *KLRK1* (**F**), and *NCR1* (**G**). Statistical analyses were performed using the log-rank test.

Table S1. List of forward and reverse primers used in qRT-PCR. Related to Star Methods

Target	Forward (F)	Reverse (R)
mActin	AGAGGGAAATCGTGCGTGAC	CAATAGTGATGACCTGGCCGT
mRpl19	GGCAGTACCCTTCCTCTTCC	AGCCTGTGACTGTCCATTCC
mCcl5	GCTGCTTTGCCTACCTCTCC	TCGAGTGACAAACACGACTGC
mIfit1	CTGAGATGTCACTTCACATGGAA	GTGCATCCCCAATGGGTTCT
mIfnβ	TCCGAGCAGAGATCTTCAGGAA	TGCAACCACCACTCATTCTGAG
hCXCL10	CCTTATCTTTCTGACTCTAAGTGGC	ACGTGGACAAAATTGGCTTG
hIFIT1	ATCCACAAGACAGAATAGCCAG	CCAGACTATCCTTGACCTGATG